Title

A comprehensive study of Interatomic Coulombic Decay in argon dimers: Extracting R-dependent absolute decay rates from the experiment

Authors

Rist, J
Miteva, T
Gaire, B
et al.

Publication Date

2017

DOI

10.1016/j.chemphys.2016.09.024

Peer reviewed

A comprehensive study of Interatomic Coulombic Decay in argon dimers: Extracting R dependent absolute decay rates from the experiment

J. Rist[1],[*] B. Gaire[2], N. Gehrken[1], M. Keiling[1,3], M. Kunitski[1], A. Moradmand[3], H. Sann[1], T. Weber[2], M. Zohrabi[7], B. Berry[7], F. Trinter[1], A. Landers[3], M. Schöffler[1], J. B. Williams[6], T. Miteva[5], P. Kolorenc[4], K. Gokhberg[5], T. Jahnke[1],[†] and R. Dörner[1][‡]

[1] *Institut für Kernphysik, Goethe Universität, Max-von-Laue-Str.1, 60438 Frankfurt, Germany*

[2] *Chemical Sciences Division, Lawrence Berkeley National Laboratory, Berkeley, CA 94720, USA*

[3] *Department of Physics, Auburn University, AL 36849, USA*

[4] *Institute of Theoretical Physics, Charles University in Prague, Prague 11636, Czech Republic*

[5] *Theoretical Chemistry Group, Heidelberg University, 69117 Heidelberg, Germany*

[6] *Department of Physics, Reno University, NV 89557, USA*

[7] *J. R. Macdonald Laboratory, Department of Physics, Kansas State University, Manhattan, KS 66506, USA*

(Dated: July 8, 2016)

Abstract

In this work we present a comprehensive and detailed study of Interatomic Coulombic Decay (ICD) occurring after irradiating argon dimers with XUV-synchrotron radiation. A manifold of different decay channels is observed and the corresponding initial and final states are assigned. Additionally, the effect of nuclear dynamics on the ICD electron spectrum is examined for one specific decay channel. The internuclear distance-dependent width $\Gamma(R)$ of the decay is obtained from the measured energy distribution employing a classical nuclear dynamics model.

[*] rist@atom.uni-frankfurt.de

[†] jahnke@atom.uni-frankfurt.de

[‡] doerner@atom.uni-frankfurt.de

I. INTRODUCTION

During the last 20 years Interatomic Coulombic Decay (ICD) has been established as a common decay mechanism of an electronic excitation in weakly bound matter. As ICD occurs, the excitation energy of one atom or molecule of a loosely bound system is transferred to a neighboring atom or molecule of the compound. The latter energy acceptor emits an electron in order to release the excess energy. After its prediction in 1997 by the Cederbaum group [1], ICD was identified in several pioneering experiments on Ne cluster [2–4] employing different experimental techniques. Followup studies during the recent years showed that ICD is not an exotic process, but rather a very common decay route in the nature as it occurs after excitation by photons [2–4], electrons [5], and ions [6] and in differently bound systems from van der Waals clusters such as the extreme case of He_2 [7] to systems consisting of hydrogen bonds such as water [8, 9]. An experimentalist point of view review of the "early years of ICD" can be found in [10] and of more recent studies in [11]. Two comprehensive theoretical review papers by Santra *et al.*[12] and Averbukh *et al.*[13] are available, as well.

ICD in argon dimers or small argon clusters has been studied in the past by employing different excitation schemes prior to ICD. In pioneering work by Morishita *et al.* ICD in argon dimers was observed after Auger decay of a $2p$-vacancy created by means of synchrotron radiation [14]. In follow up work [15–17] the occurrence of ICD in triply charged breakup channels (Ar^{++}/Ar^{+}) was examined in more detail, and as well a radiative charge transfer was observed yielding doubly charge breakup channels[18, 19]. Similar findings were reported in electron impact studies[5, 20, 21] and studies on ICD after resonant Auger decay have been reported in [22, 23].

In the present article a study of ICD at low incident photon energies is presented. A similar photon energy range (yet employing an experimentally completely different approach) was examined by Lablanquie *et al.* [24] in pioneering experiments in 2007.

II. EXPERIMENTAL SETUP

The experiment was performed using a Cold Target Recoil Ion Momentum Spectroscopy (COLTRIMS) [25–27] apparatus located at beamline 10 of the Advanced Light Source (ALS) in Berkeley operating in two-bunch mode. A beam of linearly polarized photons

of $h\nu = 51$ eV was crossed with a supersonic gas jet. The jet consisted of a mixture of 40% nitrogen and 60% argon expanding through a 30 μm nozzle at a driving pressure of 3.4 bar into vacuum. The amount of argon dimers that were generated under the given expansion conditions was on the order of a few percent. The ions and electrons created in the photo reaction were measured in coincidence by guiding them onto two separate position and time sensitive microchannel plate detectors employing an electric field of 5.6 Vcm^{-1}. A parallel magnetic field with a magnetic flux density of 7 G was superimposed in order to achieve a solid angle of detection of 4π for electrons up to 17 eV kinetic energy. The electron arm of the COLTRIMS analyzer consisted of a time-focusing scheme [27]. From the measured times-of-flight and positions of impact the 3-dimensional momentum vector of all charged fragments (and accordingly the energy and angular emission direction) was obtained.

III. RESULTS

At a photon energy of $h\nu = 51$ eV a variety of reactions may occur in the argon dimer. However, outer-valence ionization and inner-valence ionization i.e. removing a $3s$-electron, which is bound by an energy of $E = 29.3$ eV cannot trigger ICD in Ar_2, as the excitation energy of that ionized state is insufficient to further ionize the dimer. The energetically lowest lying states that can undergo ICD are Ar_2^+ shakeup states of the type $\mathrm{Ar}^{+*}(3p^4nl)$. Yet another open channel is single site direct double ionization. The double ionization ground state $(Ar^{++}(3p^4\ ^3P) - Ar)$ is located at a threshold of 43.43 eV and the first two single site doubly ionized shakeup states $(Ar^{++}(3p^4\ ^1D) - Ar)$ and $(Ar^{++}(3p^4\ ^1S) - Ar)$ can be found at energies of 45.10 eV and 47.48 eV [17].

In Fig. 1 we show how our coincident detection of both electrons and both ions can be used to unambiguously disentangle these different reactions. Fig. 1 a) depicts the energy of one of the measured electrons in dependence of the kinetic energy release (KER) of the ions. In this type of plot horizontal lines indicate photoelectrons from the population of states which can decay by ICD as their energy is independent of the KER. The first excitation levels of the singly charged $3p$-ionized Ar atom are in the range of 19.7 eV to 25.4 eV. Accordingly, photoelectron features can be expected in an energy range of 9.8 eV to 15.5 eV. However no horizontal photoelectron line is apparent in Fig. 1 a). Instead only a single broad feature is visible, which is due to the limited electron energy resolution of

our experimental setup. Furthermore a number of diagonal lines can be found, belonging to a constant sum of the electron kinetic energy and the KER. These lines occur as the excitation energy of the decaying Ar_2^{+*} is shared between the kinetic energy of the emitted electron and the two ions, which is the case, for example, in ICD.

In Fig. 1 b) the sum kinetic energy of the two electrons is depicted versus the KER. In this representation ICD can be distinguished from processes in which an additional photon is emitted. Events of ICD appear in the upper part of the figure between 12 eV and 18 eV as diagonal lines. For these events the sum energy of all fragments is a constant. The two horizontal lines located at an electron sum energy of 6 eV and 8 eV on the contrary show no dependence on the kinetic energy release. A constant sum kinetic energy of the two electrons is an evidence for double ionization of one atom of the dimer followed by an electron transfer from the other (neutral) atom and the simultaneous emission of a photon balancing the energy. According to their energy values, the two horizontal lines belong to the double ionization into the Ar_2^{++} ground state and the first excited Ar_2^{++*} state.

Fig. 1 c) shows a subset of the data presented in Fig. 1 a) with a gate on the the diagonal ICD line in Fig. 1 b). Compared to Fig. 1 a) the relative intensity in the region of high KER values of approx. 5.2 eV is significantly reduced. Using the reflection approximation [28, 29] the internuclear distance R of the two atoms at the instant of the decay can be obtained from the KER (in atomic units) by $R = 1/KER$. A value of 3.7 eV corresponds to an internuclear distance of 3.9 Å (7.4 a.u.) which is very close to the mean internuclear distance in the ground state of the argon dimer [30]. As most of the dimer shakeup states have a slightly attractive potential in the Franck-Condon region the dimer contracts during ICD. The main contribution to the decay seems to occur already at larger distances. The increased intensity at a KER of approx. 5.2 eV corresponds to a smaller internuclear distance of 2.8 Å (5.2 a.u.) indicating the inner turning point of the excited $Ar^{+*}Ar$ potential energy curve (PEC). A total of five lines are visible in Fig. 1 c) having sum energies of approximately 4.0 eV, 5.2 eV, 6.9 eV, 7.5 eV and 9.2 eV, respectively. Line (2) appears to consist of an overlap of a shorter line similar to line (3) and a longer line similar to (4) and (5). Comparing the measured energy values to the PECs shown in Fig. 2 a) the decaying states listed in Table I were assigned.

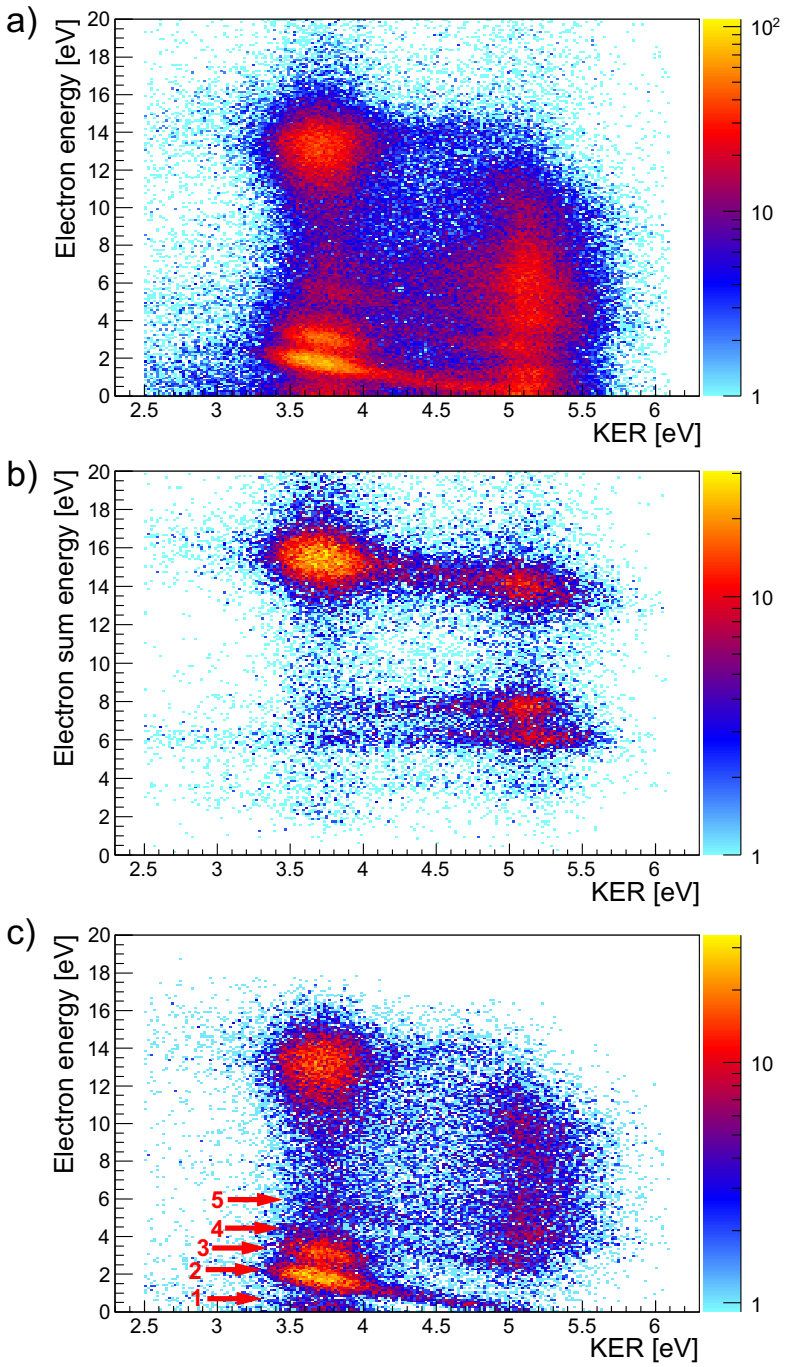

FIG. 1. (Color online) a): Energy distribution of the electron energy plotted versus kinetic energy release; b): Sum kinetic energy of the two electrons versus kinetic energy release. The diagonal lines between 12 eV and 18 eV occur due to ICD, while the horizontal lines between 4 eV and 10 eV belong to direct double ionization; c): Electron energy versus kinetic energy release with an additional restriction that the sum energy of the two electrons is between 12 eV and 18 eV.

Line	Measured sum energy [eV]	State	Calculated sum energy [eV]
(1)	4.0	$(^3P)4p\ ^2\mathbf{D}$	4.06
(2.1) long	5.2	$(^1D)4p\ ^2\mathbf{F}$	5.40
(2.2) short	5.5	$(^1D)3d\ ^2\mathbf{D}$	5.63
(3)	6.9	$(^1D)3d\ ^2\mathbf{S}$	7.07
(4)	7.5	$(^3P)4d\ ^2\mathbf{P}$	7.84
(5)	9.2	$(^1D)4d\ ^2\mathbf{S}$	9.69

TABLE I. Assignment of possible states belonging to the diagonal lines in Fig. 1 c).

The potential curves of the $Ar^{+*}(3p^{-2}4d)Ar$ states were approximated by averages of the PECs of the parent $Ar^{++}(3p^2)Ar$ states (see Ref. [31]). The potential energy curves of the remaining ionization satellites and the final two-site dicationic states of Ar_2 were computed using the configuration interaction singles doubles (CISD) method as implemented in the GAMESS-US package [32, 33]. We employed the cc-pVDZ [34] basis set augmented with four diffuse s and d, and two compact d functions [35]. In the case of the $Ar^{+*}(3p^{-2}4p)Ar$ satellites, we augmented the basis set further, adding two diffuse p functions.

For a better comparison of PECs and measured data, the electron energy is plotted versus the internuclear distance of the atoms in Fig. 2 b). The blue dashed line in Fig. 2 c) shows the Ar_2 ground state wave function. The comparison with the measured distribution highlights that for all ICD channels the dimer contracts. This is in line with the PEC shown in Fig. 2 a) which are all attractive in the Franck-Condon region.

IV. EXTRACTING THE ABSOLUTE DECAY WIDTH

From theory the decay width as function of R and the potential energy surfaces are the primary building blocks for the prediction of experimental observables like the distribution of KERs and electron kinetic energies. The interplay of nuclear dynamics and the R dependent decay width leads to the non-exponential decay of ICD and makes the KER and electron energy spectra often very sensitive probes of the absolute value of the calculated decay width. Prominent examples can be found in [38–40]). For NeAr dimers Ouchi *et al.*[41] used even the relative height of two peaks in the KER distribution to test calculated decay width very directly. Here we invert this procedure and extract absolute decay widths from our data

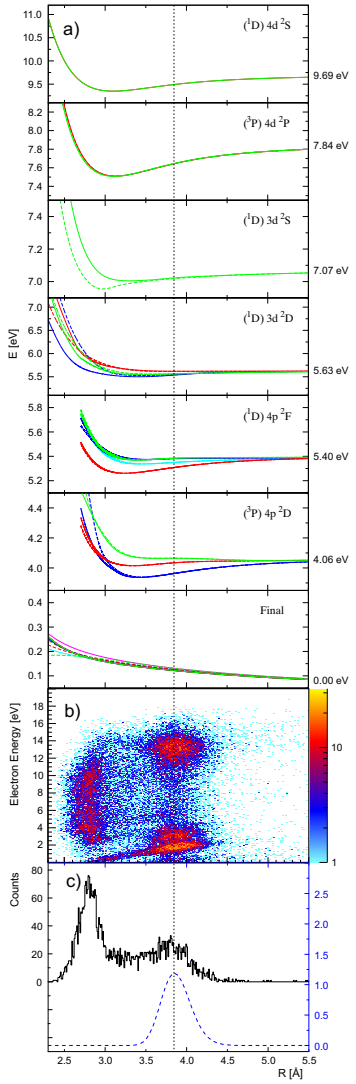

FIG. 2. (Color online) a): Potential energy curves for selected decaying states. The energy axis is shifted to the $Ar^+(3p^5) - Ar^+(3p^5)$ threshold so that it indicates the states' excess energy which is then converted into ICD electron energy and KER [36, 37]; b): Electron energy versus internuclear distance obtained within the reflection approximation (see text); c): The upper curve depicts the internuclear distance distribution of events decayed from the $(^1D)4d\ ^2S$ state (solid black). Below that the Ar_2 dimer ground state wave function density is indicated (dashed blue).

using calculated PES.

For our reverse engineering procedure, an energetically isolated state is needed for which the PEC is known and the KER-distribution must be experimentally separated from that of other states. The $(^1D)4d\ ^2S$ intermediate state satisfies this requirement. We filter events

corresponding to the $(^1D)4d\ ^2S$ intermediate state by requiring a sum kinetic energy of 8.3 eV $<$ E_{ICD} + KER $<$ 9.8 eV. For these events we calculate the internuclear distance using the reflection approximation (Fig. 2 c)).

In our inversion procedure we initiate an ensemble of n test particles with reduced mass μ with a distribution in R given by the Ar_2 dimer ground state [37] shown in the lower part of Fig. 2 c). The number of test particles n is determined by the total number of experimentally detected events i.e. the integral of the upper graph in Fig. 2 c). We discretize the R dependence of the test particle distribution in small intervals ΔR and classically propagated the test particles along the $(^1D)4d\ ^2S$ potential energy curve. The n_i particles which are located in the interval at largest R start moving inward. The residence time t_i they spend inside this interval before reaching the next one is given by the classical propagation. Accordingly the local decay rate (i.e. decays per particles per time) at this interval of R is then given by the experimentally detected decayed particles in that interval divided by the number n_i of test particles initiated within this interval and their residence time t_i.

The test particles which do not decay feed the next bin where they spend a time t_{i+1} and are added to the particles which where initialized there. These initial particles have a different (typically smaller) velocity and hence have a different residence time in that bin. The number of experimentally detected particles in that bin divided by the sum of the test particles each weighted by their respective residence time in the bin gives again the decay rate for that bin in R. Continuing this procedure results in the experimentally determined decay rates shown in Fig. 3 together with the theoretical prediction.

The latter theoretical calculation was performed using the Fano-ADC-Stieltjes method [42]. The bound and continuum parts of the resonance states as well as the coupling between them were constructed using the extended ADC(2) scheme for the one-particle propagator [43]. The basis set on each atom consisted of an effective core potential (ECP) with $4s$, $4p$, $4d$ and $1f$ basis functions with 8 active valence electrons [44]. The basis was further augmented by $8s$, $8p$, $8d$, $5f$ and $3g$ diffuse functions on the atomic centers and additional sets of $3s$, $3p$ and $4d$ functions on 5 ghost centers on the inter atomic axis. The diffuse functions were specifically designed for the computation of Rydberg and continuum states [45].

As Fig. 3 shows, the agreement between the *ab initio* calculation and the Γ_R values

extracted from the data is rather poor. This is partly in line with the findings in [41], where the *ab initio* treatment overestimated the decay width as well. However, in the present case not only the overall values differ by a factor of 10 and more, but also the qualitative slope of the R-dependence is different. At distances around and greater than 4 Å again rising values for the decay rate can be seen, which is contrary to the prediction and physical intuition. We believe those rising values to be a result from underestimating the initial particle numbers n_i at the falling edge of the ground state wave function density as well as the residence times which are calculated for zero momentum particles instead of particles with a momentum distribution. We emphasize that already around the center of the Franck-Condon region at 3.85 Å our inverting procedure is rather robust to the details of the PEC and the initial distribution. Thus we believe that disagreement between theory and experiment in this region is indeed severe. Also the fall of the experimental rates in the region below 3.7 Angstrom is very robust and our experiment thus directly confirms the strong R dependence of ICD so far only known from theory.

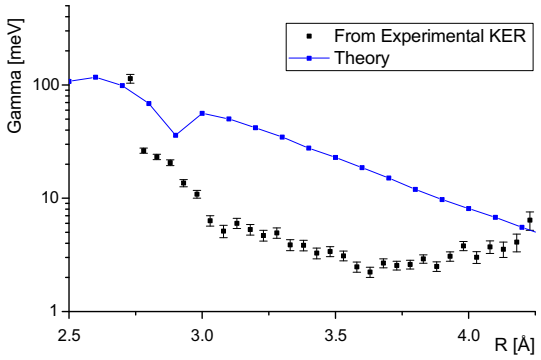

FIG. 3. (Color online) Γ extracted from KER (black squares) compared to theoretical *ab initio* calculations by P. Kolorenc (blue line) [46]. Statistical errors in Γ are indicated.

In conclusion we have given a comprehensive overview over photon induced double ionization of Ar dimers at low photon energies. The coincident detection of both electrons and KER allowed to separate radiative charge transfer following single site double ionization from the contribution of ICD following shake up single ionization. From the measured KER distribution we obtained absolute decay rates for ICD as function of internuclear distance. These decay rates show the expected strong dependence on the internuclear distance but are significantly smaller than predicted.

V. ACKNOWLEDGMENTS

This work was supported by DFG FOR1789.

---

[1] L. S. Cederbaum, J. Zobeley, and F. Tarantelli. Giant intermolecular decay and fragmentation of clusters. *Physical Review Letters*, 79(24):4778–4781, 1997.

[2] S. Marburger, O. Kugeler, U. Hergenhahn, and T. Möller. Experimental evidence for interatomic coulombic decay in ne clusters. *Physical Review Letters*, 90(20), 2003.

[3] T. Jahnke, A. Czasch, M. S. Schöffler, S. Schössler, A. Knapp, M. Käsz, J. Titze, C. Wimmer, K. Kreidi, R. E. Grisenti, A. Staudte, O. Jagutzki, U. Hergenhahn, H. Schmidt-Böcking, and R. Dörner. Experimental observation of interatomic coulombic decay in neon dimers. *Physical Review Letters*, 93(16), 2004.

[4] G. Öhrwall, M. Tchaplyguine, M. Lundwall, R. Feifel, H. Bergersen, T. Rander, A. Lindblad, J. Schulz, S. Peredkov, S. Barth, S. Marburger, U. Hergenhahn, S. Svensson, and O. Björneholm. Femtosecond Interatomic Coulombic Decay in Free Neon Clusters: Large Lifetime Differences between Surface and Bulk. *Phys. Rev. Lett.*, 93:173401, 2004.

[5] Xueguang Ren, Elias Jabbour Al Maalouf, Alexander Dorn, and Stephan Denifl. Direct evidence of two interatomic relaxation mechanisms in argon dimers ionized by electron impact. *Nature Communications*, 7:11093, 2016.

[6] J. Titze, M. S. Schoffler, H-K Kim, F. Trinter, M. Waitz, J. Voigtsberger, N. Neumann, B. Ulrich, K. Kreidi, R. Wallauer, M. Odenweller, T. Havermeier, S. Schossler, M. Meckel, L. Foucar, T. Jahnke, A. Czasch, L. Ph H. Schmidt, O. Jagutzki, R. E. Grisenti, H. Schmidt-Bocking, H. J. Ludde, and R. Dorner. Ionization dynamics of helium dimers in fast collisions with he++. *Physical review letters*, 106(3):033201, 2011.

[7] T. Havermeier, T. Jahnke, K. Kreidi, R. Wallauer, S. Voss, M. Schoffler, S. Schossler, L. Foucar, N. Neumann, J. Titze, H. Sann, M. Kuhnel, J. Voigtsberger, J. H. Morilla, W. Schollkopf, H. Schmidt-Bocking, R. E. Grisenti, and R. Dorner. Interatomic coulombic decay following photoionization of the helium dimer: observation of vibrational structure. *Physical review letters*, 104(13):133401, 2010.

[8] T. Jahnke, H. Sann, T. Havermeier, K. Kreidi, C. Stuck, M. Meckel, M. Schöffler, N. Neumann, R. Wallauer, S. Voss, A. Czasch, O. Jagutzki, A. Malakzadeh, F. Afaneh, Th. Weber, H. Schmidt-Böcking, and R. Dörner. Ultrafast energy transfer between water molecules. *Nature Physics*, 6(2):139–142, 2010.

[9] Melanie Mucke, Markus Braune, Silko Barth, Marko Förstel, Toralf Lischke, Volker Ulrich, Tiberiu Arion, Uwe Becker, Alex Bradshaw, and Uwe Hergenhahn. A hitherto unrecognized source of low-energy electrons in water. *Nature Physics*, 6(2):143–146, 2010.

[10] U. Hergenhahn. Interatomic and Intermolecular Coulombic Decay: The Early Years. *J. Electron Spectrosc. Relat. Phenom.*, 184:78, 2011.

[11] T. Jahnke. Interatomic and intermolecular Coulombic decay: the coming of age story. *J. Phys. B: Atomic, Molecular and Optical Physics*, 48:082001, 2015.

[12] R. Santra and L. S. Cederbaum. Non-Hermitian electronic theory and applications to clusters. *Phys. Reports*, 368:1, 2002.

[13] V. Averbukh, Ph. V. Demekhin, P. Kolorenc, S. Scheit, S. D. Stoychev, A. I. Kuleff, Y.-C. Chiang, K. Gokhberg, S. Kopelke, N. Sisourat, and L. S. Cederbaum. Interatomic electronic decay processes in singly and multiply ionized clusters. *J. Electron Spectrosc. Relat. Phenom.*, 183:36, 2011.

[14] Y. Morishita, X.-J. Liu, N. Saito, T. Lischke, M. Kato, G. Prümper, M. Oura, H. Yamaoka, Y. Tamenori, I. H. Suzuki, and K. Ueda. Experimental evidence of interatomic coulombic decay from the auger final states in argon dimers. *Physical Review Letters*, 96(24), 2006.

[15] K. Ueda, H. Fukuzawa, X.-J. Liu, K. Sakai, G. Prümper, Y. Morishita, N. Saito, I. H. Suzuki, K. Nagaya, H. Iwayama, M. Yao, K. Kreidi, M. Schöffler, T. Jahnke, S. Schössler, R. Dörner, Th. Weber, J. Harries, and Y. Tamenori. Interatomic coulombic decay following the auger decay: Experimental evidence in rare-gas dimers. *Journal of Electron Spectroscopy and Related Phenomena*, 166-167:3–10, 2008.

[16] *Photoemission and coincidence studies on gas-phase molecules*, volume 92 of *The 15th international conference on vacuum ultraviolet radiation physics: VUV XV*, 2008.

[17] Spas D. Stoychev, Alexander I. Kuleff, Francesco Tarantelli, and Lorenz S. Cederbaum. On the doubly ionized states of ar[sub 2] and their intra- and interatomic decay to ar[sub 2][sup 3+]. *The Journal of Chemical Physics*, 128(1):014307, 2008.

[18] N. Saito, Y. Morishita, Suzuki I. H., S. D. Stoychev, A. I. Kuleff, L. S. Cederbaum, X.-J. Liu, H. Fukuzawa, G. Prmper, and K. Ueda. Evidence of radiative charge transfer in argon dimers. *Chem. Phys. Lett*, 441:16–19, 2007.

[19] K. Ueda, X.-J. Liu, G. Prümper, H. Fukuzawa, Y. Morishita, and N. Saito. Electron–ion coincidence momentum spectroscopy: Its application to ar dimer interatomic decay. *Journal of Electron Spectroscopy and Related Phenomena*, 155(1-3):113–118, 2007.

[20] S. Yan, P. Zhang, X. Ma, S. Xu, B. Li, X. L. Zhu, W. T. Feng, S. F. Zhang, D. M. Zhao, R. T. Zhang, D. L. Guo, and H. P. Liu. Observation of interatomic coulombic decay and electron-transfer-mediated decay in high-energy electron-impact ionization of ar 2. *Physical Review A*, 88(4), 2013.

[21] Thomas Pflüger, Xueguang Ren, and Alexander Dorn. Electron-impact-induced dissociation of small argon clusters. *Physical Review A*, 91(5), 2015.

[22] K. Kimura, H. Fukuzawa, T. Tachibana, Y. Ito, S. Mondal, M. Okunishi, M. Schffler, J. Williams, Y. Jiang, Y. Tamenori, N. Saito, and K. Ueda. Controlling Low-energy Electron Emission via Resonant-Auger-induced Interatomic Coulombic Decay. *J. Phys. Chem. Lett.*, 4:1838, 2013.

[23] P. O'Keeffe, E. Ripani, P. Bolognesi, M. Coreno, M. Devetta, C. Callegari, M. Di Fraia, K. C. Prince, R. Richter, M. Alagia, A. Kivimki, and L. Avaldi. The Role of the Partner Atom and Resonant Excitation Energy in Interatomic Coulombic Decay in Rare Gas Dimers. *J. Phys. Chem. Lett.*, 4:1797, 2013.

[24] P. Lablanquie, T. Aoto, Y. Hikosaka, Y. Morioka, F. Penent, and K. Ito. Appearance of interatomic coulombic decay in ar, kr, and xe homonuclear dimers. *The Journal of Chemical Physics*, 127(15):154323, 2007.

[25] R. Dörner, V. Mergel, O. Jagutzki, L. Spielberger, J. Ullrich, R. Moshammer, and H. Schmidt-Böcking. Cold target recoil ion momentum spectroscopy: A 'momentum microscope' to view atomic collision dynamics. *Physics Reports*, 330(2-3):95–192, 2000.

[26] J. Ullrich, R. Moshammer, A. Dorn, R. D rner, L. Ph H. Schmidt, and H. Schmidt-B cking. Recoil-ion and electron momentum spectroscopy: Reaction-microscopes. *Reports on Progress in Physics*, 66(9):1463–1545, 2003.

[27] T. Jahnke, Th. Weber, T. Osipov, A. L. Landers, O. Jagutzki, L.Ph.H. Schmidt, C. L. Cocke, M. H. Prior, H. Schmidt-Böcking, and R. Dörner. Multicoincidence studies of photo and

auger electrons from fixed-in-space molecules using the coltrims technique. *Journal of Electron Spectroscopy and Related Phenomena*, 141(2-3):229–238, 2004.

[28] E. A. Gislason. Series expansions for franck-condon factors. i. linear potential and the reflection approximation. *The Journal of Chemical Physics*, 58(9):3702, 1973.

[29] L. Ph H. Schmidt, T. Jahnke, A. Czasch, M. Schoffler, H. Schmidt-Bocking, and R. Dorner. Spatial imaging of the h2(+) vibrational wave function at the quantum limit. *Physical review letters*, 108(7):073202, 2012.

[30] B. Ulrich, A. Vredenborg, A. Malakzadeh, L. Ph. H. Schmidt, T. Havermeier, M. Meckel, K. Cole, M. Smolarski, Z. Chang, T. Jahnke, and R. Dörner. Imaging of the structure of the argon and neon dimer, trimer, and tetramer. *The Journal of Physical Chemistry A*, 115(25):6936–6941, 2011.

[31] T. Miteva, Y.-C. Chiang, P. Koloren, A. I. Kuleff, K. Gokhberg, and Cederbaum L. S. Interatomic Coulombic decay following resonant core excitation of Ar in argon dimer. *J. Chem. Phys.*, 141:064307, 2014. theory.

[32] Bernard R. Brooks and Henry F. Schaefer. The graphical unitary group approach to the electron correlation problem. Methods and preliminary applications. *J. Chem. Phys.*, 70(11):5092–5106, 1979.

[33] Bernard R Brooks, William D Laidig, Paul Saxe, Nicholas C Handy, and Henry F Schaefer III. The Loop-Driven Graphical Unitary Group Approach: A Powerful Method for the Variational Description of Electron Correlation. *Phys. Scr.*, 21(3-4):312, 1980.

[34] D. E. Woon and T. H. Dunning, Jr. Gaussian basis sets for use in correlated molecular calculations. III. The atoms aluminum through argon. *J. Chem. Phys.*, 98:1358–1371, 1993.

[35] The diffuse s and d, and the compact d functions were generated as an even tempered sequence from the most diffuse s and d, and the most compact d basis functions with exponents $\xi = \alpha\beta^l$, where α is the exponent of the previous function, $\beta = 10$ and $l = 0.5$ for the compact exponent, $\beta = 10$ and $l = -0.5, -1$ for the diffuse exponents.

[36] Kirill Gokhberg. personal communication, 2013.

[37] Tsveta Miteva. personal communication, 2014.

[38] Ph. V. Demekhin, Y.-C. Chiang, S. D. Stoychev, P. Kolorenč, S. Scheit, A. I. Kuleff, F. Tarantelli, and L. S. Cederbaum. Interatomic coulombic decay and its dynamics in near following k-ll auger transition in the ne atom. *The Journal of Chemical Physics*, 131(10):104303, 2009.

[39] S. Scheit, L. S. Cederbaum, and H.-D. Meyer. Time-dependent interplay between electron emission and fragmentation in the interatomic Coulombic decay. *J. Chem. Phys.*, 118:2092, 2003. theory.

[40] N. Sisourat, N. V. Kryzhevoi, P. Koloren, S. Scheit, T. Jahnke, and L. S. Cederbaum. Ultralong-range energy transfer by interatomic Coulombic decay in an extreme quantum system. *Nature Physics*, 6:508, 2010.

[41] T. Ouchi, K. Sakai, H. Fukuzawa, I. Higuchi, Ph. V. Demekhin, Y.-C. Chiang, S. D. Stoychev, A. I. Kuleff, T. Mazza, M. Schöffler, K. Nagaya, M. Yao, Y. Tamenori, N. Saito, and K. Ueda. Interatomic coulombic decay following ne 1s auger decay in near. *Physical Review A*, 83(5), 2011.

[42] V. Averbukh and L. S. Cederbaum. Ab initio calculation of interatomic decay rates by a combination of the Fano ansatz, Green's-function methods, and the Stieltjes imaging technique. *J. Chem. Phys.*, 123:204107, 2005.

[43] F. Mertins and J. Schirmer. Algebraic propagator approaches and intermediate-state representations. i. the biorthogonal and unitary coupled-cluster methods. *Physical Review A*, 53(4):2140–2152, 1996.

[44] Andreas Nicklass, Michael Dolg, Hermann Stoll, and Heinzwerner Preuss. *Ab initio* energy-adjusted pseudopotentials for the noble gases Ne through Xe: Calculation of atomic dipole and quadrupole polarizabilities. *J. Chem. Phys.*, 102(22):8942–8952, 1995.

[45] K. Kaufmann, W. Baumeister, and M. Jungen. Universal gaussian basis sets for an optimum representation of rydberg and continuum wavefunctions. *J. Phys. B: At. Mol. Opt. Phys.*, 22(14):2223, 1989.

[46] Premysl Kolorenc. personal communication, 2014.